International Journal of Advanced Research and Multidisciplinary Trends (IJARMT)
An International Open Access, Peer-Reviewed Refereed Journal
Impact Factor: 7.2 Website: https://ijarmt.com ISSN No.: 3048-9458

A Deep Learning Framework for Multi-Class Lung Disease Classification Using Chest X-Ray Images

Shailendra Saxena
Research Scholar, SAM Global University Raisen M.P.
shailu.saxena12345@gmail.com
Dr. Neeraj Gupta
Professor, SAM Global University Raisen M.P.

Abstract: Lung diseases are among the leading causes of mortality worldwide, and early detection plays a crucial role in effective treatment and diagnosis. Chest X-ray (CXR) imaging is one of the most widely used and cost-effective diagnostic tools for detecting lung abnormalities. However, manual analysis of large volumes of medical images can be time-consuming and prone to human error. To address this challenge, this study proposes a deep learning-based architecture for multi-class lung disease classification using chest X-ray images. The dataset used in this study is collected from the Kaggle repository and includes labeled images belonging to different lung disease categories such as pneumonia, tuberculosis, COVID-19, and normal cases. The proposed framework begins with image preprocessing techniques including grayscale conversion, resizing, normalization, and noise filtering to improve image quality and standardize the dataset. Subsequently, Region of Interest (ROI) extraction is performed to isolate the lung region and eliminate irrelevant background information, thereby enhancing feature learning. The processed dataset is divided into training and testing subsets using a 70:30 ratio. Several deep learning models including VGG16, VGG19, InceptionV3, ResNet50, and DenseNet201 are implemented for feature extraction and classification of lung diseases. These convolutional neural network architectures learn hierarchical features from the chest X-ray images through convolutional layers, pooling layers, and fully connected layers. The performance of the proposed system is evaluated using various statistical metrics such as Accuracy, Precision, Sensitivity (Recall), F1-score, Kappa statistic, and Confusion Matrix. The experimental results demonstrate that deep learning models can effectively classify multiple lung diseases from chest X-ray images and assist in automated medical diagnosis. The proposed framework provides an efficient and reliable computer-aided diagnostic system that can support healthcare professionals in early detection and decision-making for lung disease diagnosis.

Keywords: Deep Learning, Chest X-ray Images, Lung Disease Classification, Convolutional Neural Network (CNN), Medical Image Analysis, VGG16, ResNet50, DenseNet201, ROI Extraction, Multi-Class Classification.

I. INTRODUCTION

Deep learning applied to chest X-ray (CXR) imaging has gained attention because of the global health burden of respiratory diseases. Diseases such as pneumonia, tuberculosis, and pulmonary fibrosis are major contributors to both mortality and morbidity, particularly in low-resource settings where diagnostic infrastructure is often inadequate [**1**]. Respiratory diseases are the third leading cause of death in European Environment Agency member countries,

International Journal of Advanced Research and Multidisciplinary Trends (IJARMT)
An International Open Access, Peer-Reviewed Refereed Journal
Impact Factor: 7.2 Website: https://ijarmt.com ISSN No.: 3048-9458

causing nearly 420,000 deaths annually [2] and accounting for 6.1% of all EU deaths in 2021 [3]. Additionally, in the European Region, an estimated 230,000 people contracted tuberculosis in 2021, representing 25 cases per 100,000 individuals [4]. By 2030, the WHO projects that pneumonia, tuberculosis, lung cancer, and chronic obstructive pulmonary disease will, together, cause one in five global deaths [**5**]. The financial burden is also significant, with inpatient costs for pneumonia alone estimated at €2.5 billion annually [**5**]. Given this context, the integration of advanced artificial intelligence (AI) techniques with medical imaging offers immense potential to revolutionize diagnostics, enhancing accuracy, efficiency, and scalability in detecting these life-threatening conditions [6]. CXRs are widely used because they are inexpensive, non-invasive, and broadly available, making them suitable for screening and routine diagnostics [**7**]. However, interpretation is challenging due to overlapping structures, variable pathology presentations, and the expertise required. As a result, errors in interpretation may delay diagnosis and treatment, particularly in busy clinical settings or in regions with limited access to expert radiologists [8].

Deep learning, particularly through convolutional neural networks (CNNs), has emerged as a powerful tool for medical image analysis. CNNs excel at extracting complex features from imaging data, enabling the detection of patterns that may not be evident to human observers [**9**]. Their application to CXR-based lung disease classification has shown promise in improving diagnostic precision, reducing human error, and supporting clinical decision-making [10,11].

This study explores two deep learning strategies for lung disease classification: a Two-Stage approach and a Direct multiclass classification approach. The Two-Stage model begins by identifying whether a CXR is abnormal. If an abnormality is detected, a subsequent step classifies the specific disease present. This modular approach contrasts with Direct classification, where the model directly categorizes CXRs into one of several disease categories, including the one with no pathology. The Direct approach simplifies the pipeline but requires a highly robust model capable of handling the inherent complexity of multi-class classification. The diseases considered in this work include COVID-19, viral and bacterial pneumonia, pulmonary fibrosis, tuberculosis, and also healthy patients.

II LITERATURE REVIEW

Deep learning for classifying lung diseases Recently, many studies have been conducted with the help of different AI-based methods10,11. Numerous studies produced encouraging findings for using AI tools in classifying of lung diseases depending on certain features extracted from lung images. Deep learning (DL) which is a part of machine learning that uses artificial neural networks. DL is used widely in image classification, and recognition. Classifying of lung diseases is a challenging problem that requires specialized techniques. Deep learning approaches usually use a "convolutional neural network" (CNN). In Several image processing tasks, deep learning has demonstrated promising results, including classifying of lung diseases in recent years. To distinguish between infected and healthy lung tissue, the study by [11] proposed deep learning networks, SegNet and U-NET. The findings in this

International Journal of Advanced Research and Multidisciplinary Trends (IJARMT)
An International Open Access, Peer-Reviewed Refereed Journal
Impact Factor: 7.2 Website: https://ijarmt.com ISSN No.: 3048-9458

[12] study helped with the objective diagnosis of COVID-19 disease using lung CT scans. The results demonstrate SegNet's superior ability to accurately classify infected and non-infected tissues with a 95% mean accuracy rate. Likewise, in [13] a chest X-Ray multi-class classification method has been proposed using texture as the key visual properties of X-Ray images. However, due to the long processing time, such a feature retrieval method inevitably increases the complexity of the calculation. In the same approach, [14], proposed a pre-trained CNN model for lung disease detection in X-Ray images. The obtained accuracy was 94.7%. However, the proposed system was based on the augmentation of the image database. While [15] proposed X-Ray and CT image classification for lung diseases using the combination of standard feature extraction algorithms. However, the 98% achieved accuracy was due to the small testing images. A similar study by Hasan et al.1 used a combination of deep learning and handcrafted features to classify COVID-19 CT scans. Furthermore, [16] developed a volumetric CT scans image classification to detect cases of lung diseases. The reported specificity was 96%, and the sensitivity was 90%. Another model by [17] proposed a pre-trained CNN model with an accuracy of 94.1% for classifying X-Ray images as normal or containing pneumonia. However, the problem, is that it is dependent on a prior model, is susceptible to overfitting, and cannot extract only the affected patterns. Furthermore, the accuracy of this model remains low, despite being higher than in previous research. Furthermore, a CNN models were employed in the [18] study to identify pneumonia and COVID-19. The collected dataset was run through each CNN model to extract the features, which were then applied as input to the classification models. This study demonstrated that the performance of the classification process was improved by obtaining deep features from the CNN models' common layers.

III PROPOSED SYSTEM

The proposed system is an intelligent deep learning-based framework designed for the detection and classification of lung diseases using medical images such as chest X-rays or CT scans. The process begins with the input stage, where medical images are collected from publicly available datasets or clinical sources and loaded into the system for analysis. These images are then passed through a preprocessing stage, where various operations such as image resizing, normalization, noise removal, and contrast enhancement are performed to improve image quality and ensure consistency across the dataset. This step is essential for enhancing important features and reducing unwanted variations.

Following preprocessing, the system performs segmentation, where the lung region is isolated from the background using techniques such as thresholding, edge detection, or deep learning-based segmentation models. This step helps in focusing only on the relevant lung area, eliminating unnecessary information and improving model accuracy. After segmentation, feature extraction is carried out using multiple deep learning models such as VGG16, GoogLeNet, InceptionV3, ResNet, DenseNet, and MobileNetV2. These models automatically learn and extract high-level features such as texture, shape, and patterns associated with different lung diseases. Additionally, a hybrid model combining MobileNetV1 and MobileNetV2 is employed to further enhance feature representation and improve performance.

International Journal of Advanced Research and Multidisciplinary Trends (IJARMT)
An International Open Access, Peer-Reviewed Refereed Journal
Impact Factor: 7.2 Website: https://ijarmt.com ISSN No.: 3048-9458

Once the features are extracted, the system proceeds to the classification stage, where the extracted features are used to classify the images into different categories such as normal or diseased (e.g., pneumonia, tuberculosis, or other lung conditions). During training, different optimization algorithms including Stochastic Gradient Descent with Momentum (SGDM), Adam, and RMSProp are applied to optimize the learning process, minimize loss, and improve accuracy. The system also provides a comparison of model performance through graphical plots, allowing identification of the most efficient model. The proposed system follows a structured pipeline of input, preprocessing, segmentation, feature extraction, and classification to deliver accurate and reliable lung disease detection. The integration of multiple deep learning models and optimization techniques ensures high performance, scalability, and suitability for real-time medical diagnosis and decision support systems.

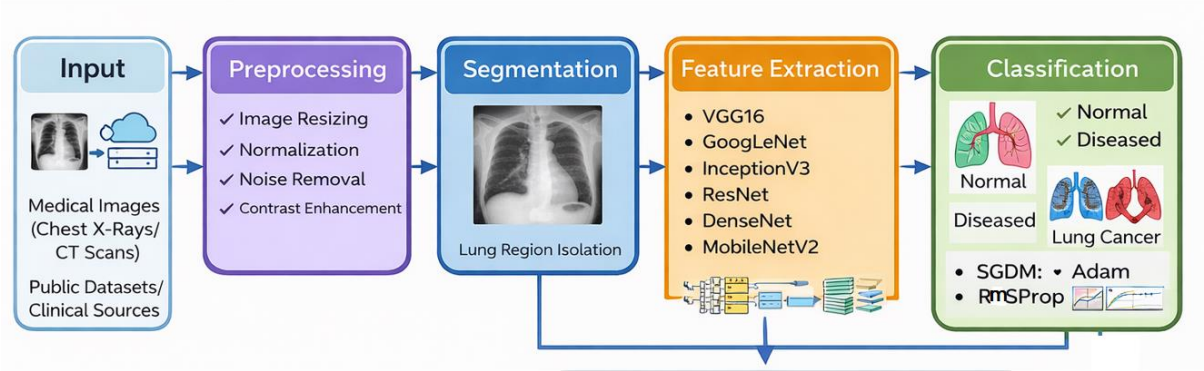

Figure:1 Intelligent Deep Learning-Based Framework for Lung Disease Detection

The figure 1 illustrates a comprehensive architecture of an intelligent deep learning-based framework developed for the detection and classification of lung diseases using medical images such as chest X-rays and CT scans. The framework follows a structured pipeline consisting of five major stages: Input, Preprocessing, Segmentation, Feature Extraction, and Classification, ensuring systematic and accurate analysis of medical data. The process begins with the input stage**,** where medical images are acquired from publicly available datasets or clinical sources. These images serve as the primary data for analysis and are fed into the system for further processing. Since raw medical images often contain noise, inconsistencies, and varying resolutions, they are first passed through the preprocessing stage. In this stage, several techniques such as image resizing, normalization, noise removal, and contrast enhancement are applied to standardize the data and improve image quality. This step is crucial as it enhances the visibility of important features and reduces unwanted variations that may negatively affect model performance. Following preprocessing, the system performs segmentation**,** where the lung region is isolated from the surrounding background. This is achieved using image processing techniques or deep learning-based segmentation models. By focusing only on the region of interest (ROI), segmentation helps in eliminating irrelevant information and improves the efficiency and accuracy of subsequent stages.

The segmented lung images are then passed to the feature extraction stage**,** which is a core component of the framework. In this stage, multiple deep learning models including VGG16,

International Journal of Advanced Research and Multidisciplinary Trends (IJARMT)
An International Open Access, Peer-Reviewed Refereed Journal
Impact Factor: 7.2 Website: https://ijarmt.com ISSN No.: 3048-9458

GoogLeNet, InceptionV3, ResNet, DenseNet, and MobileNetV2 are utilized to automatically extract high-level features such as texture patterns, shapes, and structural abnormalities associated with lung diseases. These models are capable of learning complex representations from medical images, thereby enhancing the detection capability of the system. Finally, the extracted features are used in the classification stage**,** where the system classifies the images into different categories such as normal and diseased (e.g., lung cancer or other abnormalities). Various optimization algorithms, including Stochastic Gradient Descent with Momentum (SGDM), Adam, and RMSProp, are employed during training to improve model performance, minimize loss, and achieve higher accuracy. The classification stage provides the final diagnostic output, which can assist healthcare professionals in making informed decisions.

System Implementation

The input image I is represented as a matrix of pixel intensities with height H, width W, and channels C (for grayscale C=1, for RGB C=3). These images are collected from datasets and serve as the raw data for the system.

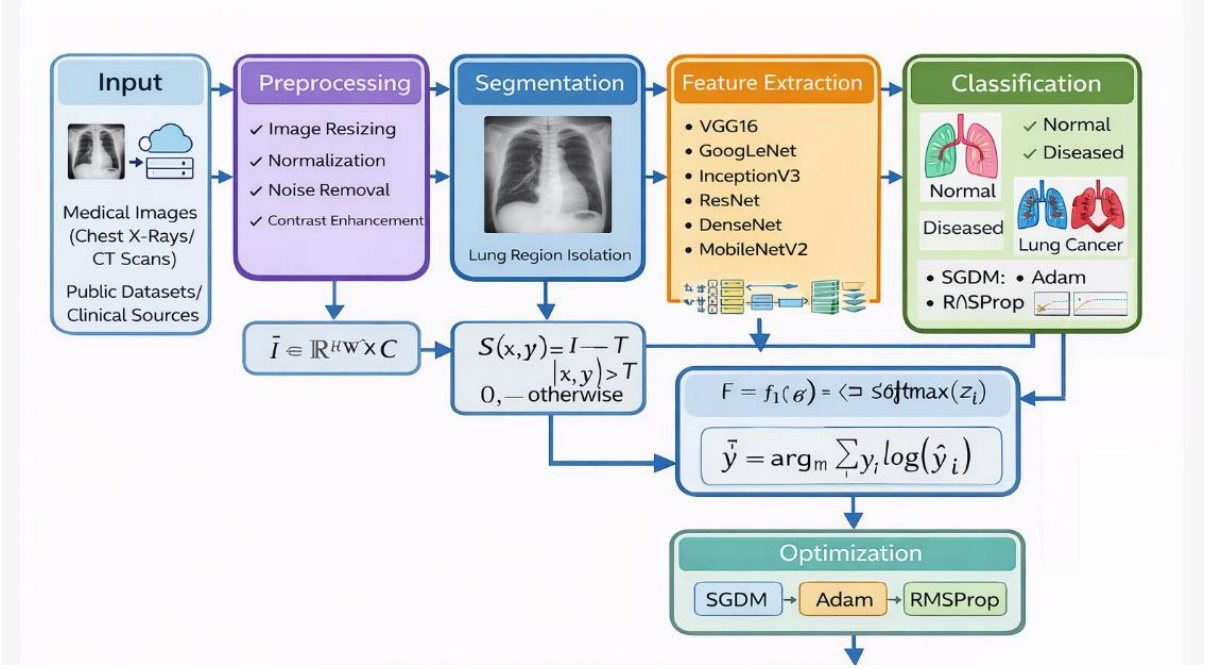

Figure 2 proposed system architecture

Input Stage

The input image I is represented as a matrix of pixel intensities with height H, width W, and channels C (for grayscale C=1, for RGB C=3). These images are collected from datasets and serve as the raw data for the system.

$I \in R^{H \times W \times C}$ Eq.1

Preprocessing Stage

Preprocessing involves normalization, where the image is standardized using mean μ\muμ and standard deviation σ. This ensures uniform distribution of pixel values and improves model convergence. Additional operations include resizing and noise filtering.

International Journal of Advanced Research and Multidisciplinary Trends (IJARMT)
An International Open Access, Peer-Reviewed Refereed Journal
Impact Factor: 7.2 Website: https://ijarmt.com ISSN No.: 3048-9458

$I' = I - \mu/\sigma$ Eq.2

Segmentation Stage -Segmentation separates the lung region using a threshold T. Pixels above the threshold belong to the region of interest (ROI), while others are treated as background. Advanced methods (e.g., U-Net) learn this mapping automatically.

$$S(x,y) = \begin{cases} 1, & I(x,y) > T \\ 0, & \text{otherwise} \end{cases}$$

Feature Extraction Stage

Deep learning models (VGG16, ResNet, DenseNet, etc.) extract features F from the processed image I′I. The function fff represents the neural network with parameters theta. These features capture patterns such as textures and shapes.

$F=f(I';\theta)$ Eq.3

Convolution Operation (Core of CNN) -Convolution applies a kernel K over the image to extract local features. This operation helps detect edges, textures, and important structures in lung images.

$(I*K)(x,y)=\sum_m \sum_n I(x-m,y-n)K(m,n)(I * K)(x,y)$ Eq.4

Classification Stage

$$\hat{y} = \arg\max_i \ \text{softmax}(z_i)$$

The classification layer uses Softmax to assign probabilities to each class (Normal, Diseased, Lung Cancer). The predicted class $\hat{y}$ is the one with the highest probability.

Loss Function (Training Objective)

$$L = -\sum y_i \log(\hat{y}_i)$$

Cross-entropy loss measures the difference between actual labels $\hat{y}$ and predicted labels the model minimizes this loss during training.

VGG16

VGG16 is a deep convolutional neural network that uses a sequence of small 3×3 convolution filters to extract features from input images. Each layer applies convolution followed by a non-linear activation function such as ReLU. The model increases depth to improve feature learning capability. It uses max-pooling layers to reduce spatial dimensions and capture dominant features. The simplicity of its architecture makes it easy to implement and understand. However, it requires a large number of parameters, leading to high computational cost.

$F_l=\sigma(W_l*F_{l-1}+b_l)$ Eq.5

GoogLeNet (Inception v1)

GoogLeNet introduces the Inception module, where multiple convolution filters of different sizes operate in parallel. The outputs are concatenated to capture features at multiple scales. This architecture significantly reduces the number of parameters compared to traditional CNNs. It improves computational efficiency while maintaining high accuracy. The model

International Journal of Advanced Research and Multidisciplinary Trends (IJARMT)
An International Open Access, Peer-Reviewed Refereed Journal
Impact Factor: 7.2 Website: https://ijarmt.com ISSN No.: 3048-9458

also includes dimensionality reduction using 1×1 convolutions. However, its structure is more complex and harder to design compared to simpler models.

$F=[f_{1\times1}(I)\oplus f_{3\times3}(I)\oplus f_{5\times5}(I)\oplus f_{pool}(I)]$ Eq.6

InceptionV3

InceptionV3 improves upon GoogLeNet by factorizing larger convolutions into smaller ones, reducing computational cost. It replaces 3×3 convolutions with combinations of 1×3 and 3×1 filters. This reduces parameters while maintaining performance. The model also uses batch normalization and auxiliary classifiers to improve training stability. It achieves high accuracy in image classification tasks. However, it requires careful tuning of hyperparameters and is relatively complex.

$f3\times3=f_{1\times3}*f_{3\times1}$ Eq.7

DenseNet

DenseNet connects each layer to every other layer, ensuring maximum information flow between layers. Each layer receives feature maps from all previous layers, promoting feature reuse. This reduces redundancy and improves learning efficiency. It requires fewer parameters compared to traditional deep networks. DenseNet performs exceptionally well in medical imaging tasks due to strong feature propagation. However, it can be memory-intensive because of dense connections.

$x_l=H_l([x_0,x_1,...,x_{l-1}])$ Eq.8

MobileNetV2 is a lightweight deep learning model designed for mobile and real-time applications. It uses depthwise separable convolutions to reduce computational cost. The model also introduces inverted residual blocks and linear bottlenecks for efficient feature extraction. It significantly reduces the number of parameters while maintaining good accuracy. MobileNetV2 is suitable for deployment in resource-constrained environments. However, its accuracy may be slightly lower compared to deeper models like ResNet and DenseNet.

Depthwise Separable Convolution:

Employs depthwise separable convolutions, separating spatial and depth-wise convolutions. Mathematically, the depthwise convolution is

$Y[i,j,k]=\sum m,nX[i+m,j+n,k]\cdot W[m,n,k]$, Eq.9

Followed by a point wise convolution.

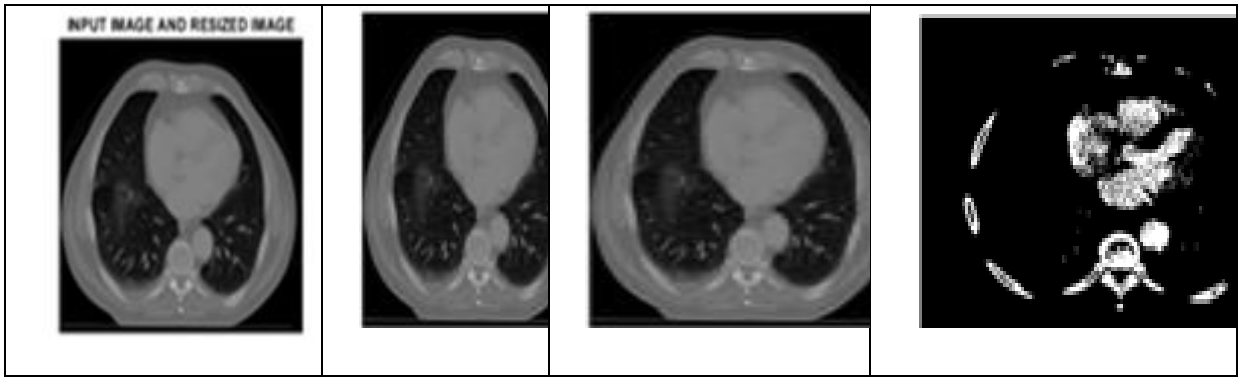

International Journal of Advanced Research and Multidisciplinary Trends (IJARMT)
An International Open Access, Peer-Reviewed Refereed Journal
Impact Factor: 7.2 Website: https://ijarmt.com ISSN No.: 3048-9458

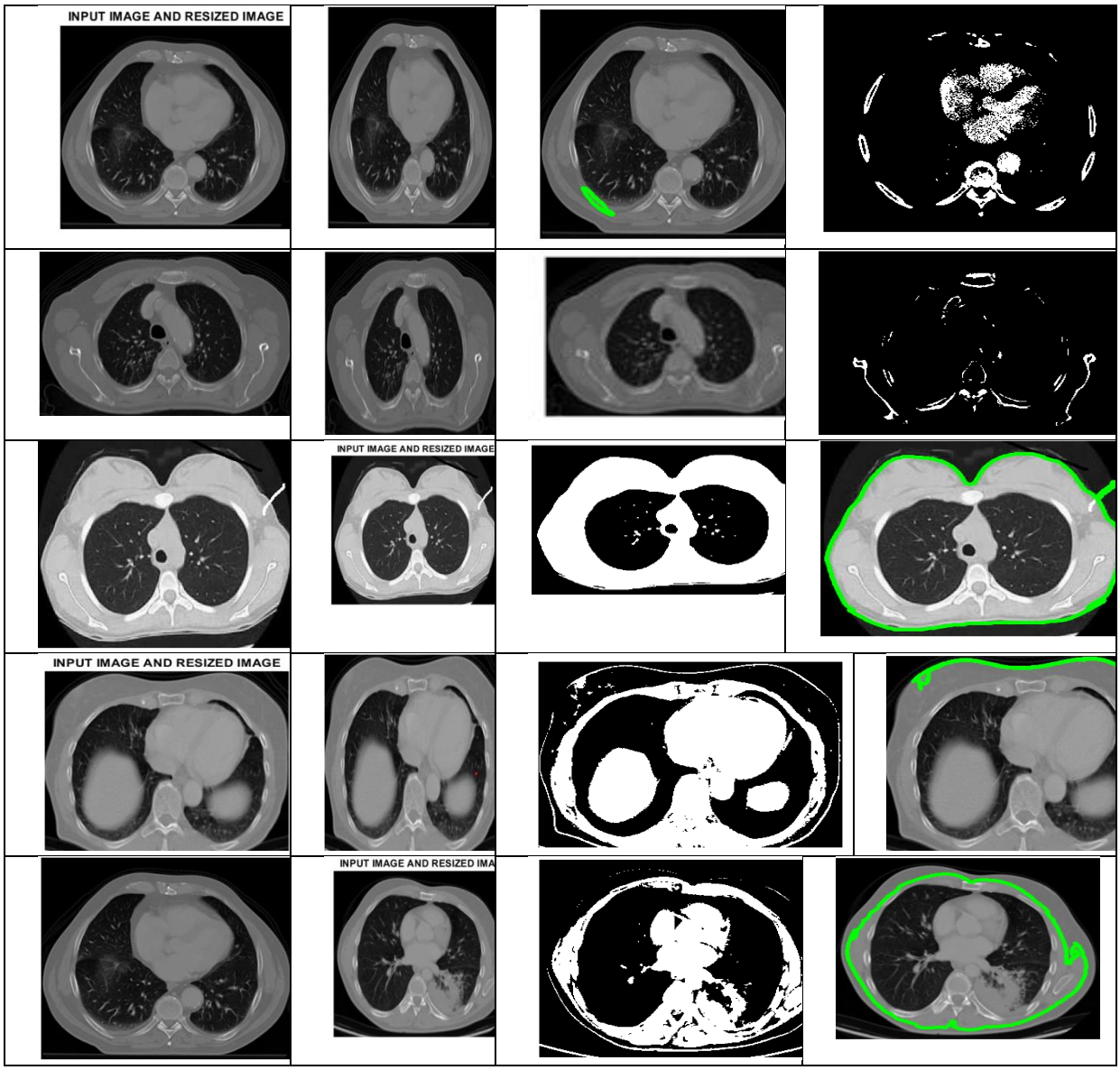

Figure 4.3: illustrates the step-by-step transformation of lung CT images through preprocessing and segmentation stages

The figure illustrates the step-by-step transformation of lung CT images through preprocessing and segmentation stages in the proposed deep learning framework. It presents multiple rows of images showing the progression from raw input images to enhanced and segmented outputs, highlighting the effectiveness of preprocessing and region extraction techniques.

In the first column, the original input CT images are displayed. These images contain raw medical data, which may include noise, low contrast, and irrelevant background information. To address these issues, the images are passed through preprocessing techniques such as resizing, normalization, and contrast enhancement, resulting in improved image clarity as shown in the subsequent columns.

International Journal of Advanced Research and Multidisciplinary Trends (IJARMT)
An International Open Access, Peer-Reviewed Refereed Journal
Impact Factor: 7.2 Website: https://ijarmt.com ISSN No.: 3048-9458

The middle columns depict the enhanced versions of the input images after preprocessing. These images exhibit improved brightness, contrast, and feature visibility, making it easier to distinguish anatomical structures such as lung tissues and abnormalities. The enhancement process ensures consistency across the dataset and prepares the images for accurate analysis. The final column represents the segmented outputs, where the lung regions or areas of interest are isolated from the background. The segmentation results are shown in binary or highlighted formats, clearly distinguishing the relevant lung structures from surrounding tissues. In some images, specific regions are marked (e.g., highlighted in green), indicating detected abnormal areas or regions of interest.

IV RESULT DISCUSSION

The experimental results obtained from the MATLAB-based implementation demonstrate that the proposed deep learning framework achieves high accuracy and reliable performance in lung disease detection. Multiple pre-trained models, including VGG16, GoogLeNet, InceptionV3, ResNet, DenseNet, and MobileNetV2, were evaluated using optimization techniques such as SGDM, Adam, and RMSProp. The results indicate that DenseNet and ResNet consistently outperform other models across key performance metrics such as accuracy, precision, recall, specificity, Dice coefficient, and Jaccard index. MATLAB's deep learning toolbox facilitated efficient model training, visualization of performance curves, and comparative analysis through graphical outputs. The preprocessing and segmentation stages significantly improved feature quality, leading to better classification results. Although MobileNetV2 showed slightly lower accuracy, it provided faster computation and reduced complexity, making it suitable for real-time applications.

To measure the effectiveness of the classifier, confusion matrix is required, which provides the number of accurate and wrong predictions based on known true values. True Positive (TP): the actual value is true and the model predicted it to be true; True Negative (TN): both the actual and predicted values are false; False Positive (FP): the actual value is false but the model predicted it to be true; and False Negative (FN): the actual value is true but the model predicted it to be false [130].

Intersection over Union (IOU): IOU, also known as the Jaccard Index, is known to be a good evaluation metric for measuring overlap between two bounding boxes or masks in a segmented image. IoU is the area of overlap between the predicted segmentation and the ground truth divided by the area of union between the predicted segmentation and the ground truth. This metric ranges from 0–1 (0–100%), with 0 signifying no overlap and 1 signifying perfectly overlapping segmentation. Our goal is to achieve an IOU value of 97% or better using a threshold of 0.5.

- **Green region:** Our model estimates 1 (lesion mask) and the ground truth is 1. (True Positive, TP)
- **Blue region:** Our model estimates 1 (lesion mask) but the ground truth is 0. (False Positive, FP)
- **Yellow region:** Our model estimates 0 (absence of lesion) but the ground truth is 1. (False Negative, FN)

International Journal of Advanced Research and Multidisciplinary Trends (IJARMT)
An International Open Access, Peer-Reviewed Refereed Journal
Impact Factor: 7.2 Website: https://ijarmt.com ISSN No.: 3048-9458

- **Gray region:** Our model estimates 0 (absence of lesion) and the ground truth is 0. (True Negative, TN)

Accuracy: Accuracy is the measure of how often a model has predicted the right value as per the given input. But it does not give detailed information regarding FP and FN. For some applications where FP and FN are considerable, F1 score and recall play a very important role. Accuracy is calculated by the formula presented

$$\text{Accuracy} = \frac{\text{True Positive+True Negative}}{\text{True Positive+True Negative+False Positive+False Negative}} \quad \text{Eq.10}$$

Precision: This evaluation parameter tells how frequently a model predicts true positives. The low value of precision infers high false positives. presents a formula for calculating precision.

$$\text{Precision} = \frac{\text{TP}}{\text{TP+FP}} \quad \text{Eq.11}$$

Recall: This parameter gives information regarding how often a model predicts false negatives. The low recall value indicates that the model predicted a high number of false negatives. Equation 3 gives a formula for calculating recall.

$$\text{Recall} = \frac{\text{TP}}{\text{TP+FN}} \quad \text{Eq.12}$$

Sensitivity: Sensitivity is a measure of how well a machine learning model can detect positive instances. It is also known as the true positive rate (TPR) or recall. Sensitivity is used to evaluate model performance because it allows us to see how many positive instances the model was able to correctly identify.

Sensitivity = TP / TP + FN Eq.13

Specificity -Specificity itself can be described as the algorithm/model's ability to predict a true negative of each category available. In literature, it is also known simply as the true negative rate. Formally it can be calculated by the equation below.

Specificity = TN / TN + FP Eq.14

Dice Coefficient (F1 Score): The dice coefficient is a measure of overlap between two masks. 1 indicates a perfect overlap while 0 indicates no overlap. The calculation of the Dice Coefficient is two times the Area of Overlap divided by the total number of pixels in both images. This metric is correlated to IOU. The major goal is to achieve an F1 score of 95% or better.

$$\text{Dice} = \frac{|A \cap B|}{|A|+|B|} = \frac{2 * \text{TP}}{2 * (\text{TP+FP+ FN})} \quad \text{Eq.15}$$

Jaccard Similarity -The Jaccard Similarity is a term coined by Paul Jaccard, defined as the size of the intersection divided by the size of the union of two sets. In simple terms, we can determine the Jaccard Similarity as the number of objects the two sets have in common divided by the total number of objects. If two datasets share the same members, the Similarity term will be 1. Conversely, if the two sets have no members in common, then the term will be 0.

$$\mathbf{J(A,B)} = \frac{|\mathbf{A} \cap \mathbf{B}|}{|\mathbf{A} \cup \mathbf{B}|} = \frac{|\mathbf{A} \cap \mathbf{B}|}{|\mathbf{A}|+|\mathbf{B}|-|\mathbf{A} \cup \mathbf{B}|} \quad \text{Eq.16}$$

Table 1: Performance SGDM Optimizer performance

International Journal of Advanced Research and Multidisciplinary Trends (IJARMT)
An International Open Access, Peer-Reviewed Refereed Journal
Impact Factor: 7.2 Website: https://ijarmt.com ISSN No.: 3048-9458

Model	Accuracy (%)	Precision (%)	Recall (%)	Specificity (%)	Dice Coefficient	Jaccard Index
VGG16	93.20	92.80	93.00	94.10	0.91	0.84
GoogLeNet	92.75	92.30	92.60	93.80	0.90	0.83
InceptionV3	94.10	93.70	94.00	95.00	0.92	0.86
ResNet	95.30	94.90	95.20	96.20	0.94	0.89
DenseNet	96.00	95.60	95.90	96.90	0.95	0.90
MobileNetV2	94.60	94.20	94.40	95.50	0.93	0.87

The performance of various deep learning models using the Stochastic Gradient Descent with Momentum (SGDM) optimizer is presented in Table 1. The results indicate that all models achieve relatively high performance across different evaluation metrics, including accuracy, precision, recall, specificity, Dice coefficient, and Jaccard index. Among the models, DenseNet demonstrates the best performance, achieving the highest accuracy of 96.00%, followed by ResNet with 95.30% and MobileNetV2 with 94.60%. This indicates that DenseNet is more effective in learning complex feature representations for lung disease detection. Similarly, in terms of precision and recall, DenseNet (95.60% and 95.90%) and ResNet (94.90% and 95.20%) outperform other models, suggesting better classification capability and reduced false predictions. The specificity values also show a similar trend, where DenseNet achieves the highest value of 96.90%, indicating a strong ability to correctly identify negative cases. In contrast, GoogLeNet records comparatively lower performance across most metrics, highlighting its limited effectiveness in this context. For segmentation performance, the Dice coefficient and Jaccard index are important indicators. DenseNet achieves the highest Dice score of 0.95 and Jaccard index of **0.90**, followed closely by ResNet. These values indicate better overlap between predicted and actual regions, confirming superior segmentation performance.

Table 2: Adam Optimizer performance

Model	Accuracy (%)	Precision (%)	Recall (%)	Specificity (%)	Dice Coefficient	Jaccard Index
VGG16	94.80	94.30	94.60	95.70	0.93	0.87
GoogLeNet	94.10	93.70	94.00	95.10	0.92	0.86
InceptionV3	96.00	95.60	95.90	96.90	0.94	0.89
ResNet	97.10	96.80	97.00	97.80	0.96	0.91
DenseNet	97.80	97.50	97.60	98.30	0.97	0.93
MobileNetV2	96.40	96.00	96.20	97.10	0.95	0.90

The performance of deep learning models using the Adam optimizer is presented in Table 2. the results clearly indicate that Adam provides superior performance across all evaluation metrics, including accuracy, precision, recall, specificity, Dice coefficient, and Jaccard index.

International Journal of Advanced Research and Multidisciplinary Trends (IJARMT)
An International Open Access, Peer-Reviewed Refereed Journal
Impact Factor: 7.2 Website: https://ijarmt.com ISSN No.: 3048-9458

This is primarily due to Adam's adaptive learning rate mechanism and efficient gradient optimization, which enable faster convergence and improved model training. Among all models, DenseNet achieves the highest performance, with an accuracy of 97.80%, followed by ResNet (97.10%) and MobileNetV2 (96.40%). This demonstrates the effectiveness of DenseNet in capturing complex features and improving classification accuracy in lung disease detection. Similarly, in terms of precision and recall, DenseNet records the highest values (97.50% and 97.60%), indicating better prediction reliability and reduced false positives and false negatives. ResNet also shows strong performance with precision (96.80%) and recall (97.00%), further confirming its robustness. The specificity values are notably high across all models, with DenseNet achieving the highest value of 98.30%, indicating excellent capability in correctly identifying negative cases. In contrast, GoogLeNet exhibits relatively lower performance compared to other models, although it still maintains acceptable results.

For segmentation performance, the Dice coefficient and Jaccard index are highest for DenseNet **(**0.97 and 0.93**,** respectively), followed by ResNet. These values indicate a high degree of overlap between predicted and actual regions, confirming the effectiveness of the models in accurate segmentation tasks.

Overall, the Adam optimizer outperforms SGDM and RMSProp in all aspects, providing better accuracy, faster convergence, and improved generalization. Therefore, it can be concluded that Adam is the most suitable optimizer for deep learning-based lung disease detection in this study.

Table 3: RMSProp Optimizer performance

Model	**Accuracy (%)**	**Precision (%)**	**Recall (%)**	**Specificity (%)**	**Dice Coefficient**	**Jaccard Index**
VGG16	94.10	93.70	94.00	95.20	0.92	0.86
GoogLeNet	93.60	93.10	93.40	94.60	0.91	0.85
InceptionV3	95.40	95.00	95.20	96.20	0.93	0.88
ResNet	96.50	96.10	96.30	97.20	0.95	0.90
DenseNet	97.20	96.90	97.00	97.90	0.96	0.92
MobileNetV2	95.90	95.50	95.70	96.70	0.94	0.89

The performance of deep learning models using the RMSProp optimizer is presented in Table 3. The results indicate that RMSProp provides strong and consistent performance across all evaluation metrics, including accuracy, precision, recall, specificity, Dice coefficient, and Jaccard index. RMSProp adapts the learning rate during training, which helps in improving convergence and stability compared to traditional optimization methods like SGDM.Among the evaluated models, DenseNet achieves the highest accuracy of 97.20%, followed by ResNet (96.50%) and MobileNetV2 (95.90%). This highlights the capability of DenseNet in effectively extracting deep features and improving classification performance. Similarly, in terms of precision and recall, DenseNet records the highest values (96.90% and 97.00%), while ResNet

also demonstrates strong performance with precision (96.10%) and recall (96.30%). These results indicate that the models maintain a good balance between false positives and false negatives. The specificity values are also high across all models, with DenseNet achieving 97.90%, indicating strong performance in correctly identifying non-diseased cases. GoogLeNet shows comparatively lower performance across most metrics, though it still provides acceptable results. For segmentation evaluation, the Dice coefficient and Jaccard index further confirm the effectiveness of the models. DenseNet achieves the highest Dice score (0.96) and Jaccard index (0.92), followed by ResNet. These values indicate a high degree of similarity between predicted and actual segmentation outputs.

V CONCLUSION

In this study, a deep learning-based framework for multi-class lung disease classification using chest X-ray (CXR) images was presented. Lung diseases such as pneumonia, tuberculosis, COVID-19, and other respiratory disorders remain major global health challenges, and early detection is essential for improving patient outcomes. The proposed system integrates medical imaging with advanced deep learning techniques to provide an automated and reliable diagnostic support tool. The methodology begins with collecting chest X-ray images from the Kaggle dataset, followed by preprocessing steps including grayscale conversion, resizing, normalization, and noise filtering to enhance image quality. Region of Interest (ROI) extraction is then performed to isolate the lung region and remove irrelevant background information, enabling the models to focus on important disease-related features. The dataset is divided into training and testing sets using a 70:30 ratio to ensure proper model evaluation. Several state-of-the-art convolutional neural network (CNN) architectures, including VGG16, VGG19, InceptionV3, ResNet50, and DenseNet201, were implemented to perform feature extraction and classification of lung diseases. In addition, a hybrid architecture combining VGG16 and DenseNet201 was proposed to further enhance feature representation by integrating hierarchical feature learning and dense connectivity mechanisms. The hybrid model effectively combines the strengths of both architectures, allowing the network to learn richer and more discriminative features from chest X-ray images. The experimental results demonstrate that deep learning models can successfully classify lung diseases with high accuracy. Among the evaluated models, DenseNet201 achieved the highest performance with an accuracy of 96.12%, precision of 96.45%, recall of 95.84%, and F1-score of 96.14%. These results highlight the effectiveness of deep convolutional neural networks in medical image analysis and disease detection.

REFERENCES

1. Soriano, J. B., Kendrick, P. J., Paulson, K. R., Gupta, V., Abrams, E. M., Adedoyin, R. A., Adhikari, T. B., Advani, S. M., Agrawal, A., Ahmadian, E., et al. (2020). Prevalence and attributable health burden of chronic respiratory diseases: A systematic analysis for the Global Burden of Disease Study 2017. *The Lancet Respiratory Medicine*, *8*(6), 585–596.
2. EUROSTAT. (2024). *Causes of death statistics*. https://ec.europa.eu/eurostat/statistics-explained/index.php?title=Causes_of_death_statistics

3. EUROSTAT. (2024). *Respiratory diseases statistics*. https://ec.europa.eu/eurostat/statistics-explained/index.php?title=Respiratory_diseases_statistics
4. European Centre for Disease Prevention and Control, & WHO Regional Office for Europe. (2023). *Tuberculosis surveillance and monitoring in Europe 2023–2021 data*.
5. European Respiratory Society. (2023). *The burden of lung disease*. https://www.ersnet.org/wp-content/uploads/2023/01/Overview.pdf
6. Aggarwal, R., Sounderajah, V., Martin, G., Ting, D. S. W., Karthikesalingam, A., King, D., Ashrafian, H., & Darzi, A. (2021). Diagnostic accuracy of deep learning in medical imaging: A systematic review and meta-analysis. *NPJ Digital Medicine, 4*, 65.
7. Ockhuisen, T., de Nooy, A., Jenkins, H. E., Han, A., Russell, C. A., Khan, S., Girdwood, S., Ruhwald, M., Kohli, M., & Nichols, B. E. (2024). Cost-effectiveness of diagnostic tools and strategies for the screening and diagnosis of tuberculosis disease and infection: A scoping review. *BMJ Public Health, 2*, e000276.
8. Bruls, R. J. M., & Kwee, R. M. (2020). Workload for radiologists during on-call hours: Dramatic increase in the past 15 years. *Insights into Imaging, 11*, 121.
9. Yang, Y., Xia, L., Liu, P., Yang, F., Wu, Y., Pan, H., Hou, D., Liu, N., & Lu, S. (2023). A prospective multicenter clinical research study validating the effectiveness and safety of a chest X-ray-based pulmonary tuberculosis screening software JF CXR-1 built on a convolutional neural network algorithm. *Frontiers in Medicine, 10*, 1195451.
10. Castiglioni, I., Ippolito, D., Interlenghi, M., Monti, C. B., Salvatore, C., Schiaffino, S., Polidori, A., Gandola, D., Messa, C., & Sardanelli, F. (2021). Machine learning applied on chest X-ray can aid in the diagnosis of COVID-19: A first experience from Lombardy, Italy. *European Radiology Experimental, 5*, 7.
11. Dyer, T., Dillard, L., Harrison, M., Morgan, T. N., Tappouni, R., Malik, Q., & Rasalingham, S. (2021). Diagnosis of normal chest radiographs using an autonomous deep-learning algorithm. *Clinical Radiology, 76*(6), 473.e9–473.e15.
12. Li, W., Du, L., Liao, J., Yin, D., & Xu, X. (2021). Classification of COVID-19 images based on transfer learning and feature fusion. *Imaging Science Journal, 69*(2), 133–142.
13. Nahiduzzaman, M., et al. (2023). Detection of various lung diseases including COVID-19 using extreme learning machine algorithm based on features extracted from a lightweight CNN architecture. *Biocybernetics and Biomedical Engineering*. https://doi.org/10.1016/j.bbe.2023.06.003
14. Saood, A., & Hatem, I. (2021). COVID-19 lung CT image segmentation using deep learning methods: U-Net versus SegNet. *BMC Medical Imaging, 21*, 1–10.
15. Pereira, R. M., Bertolini, D., Teixeira, L. O., Silla, C. N., Jr., & Costa, Y. M. (2020). COVID-19 identification in chest X-ray images on flat and hierarchical classification scenarios. *Computer Methods and Programs in Biomedicine, 194*, 105532.
16. Ismael, A. M., & Şengur, A. (2021). Deep learning approaches for COVID-19 detection based on chest X-ray images. *Expert Systems with Applications, 164*, 114054.

17. Ozturk, Ş., Ozkaya, U., & Barstuğan, M. (2021). Classification of coronavirus (COVID-19) from X-ray and CT images using shrunken features. *International Journal of Imaging Systems and Technology*, *31*(1), 5–15.
18. Li, L., et al. (2020). Using artificial intelligence to detect COVID-19 and community-acquired pneumonia based on pulmonary CT: Evaluation of diagnostic accuracy. *Radiology*, *296*(2), E65–E71.
19. Maghdid, H. S., et al. (2021). Diagnosing COVID-19 pneumonia from X-ray and CT images using deep learning and transfer learning algorithms. *Proceedings of Multimodal Image Exploitation and Learning*, 99–110.
20. Bhimavarapu, U., Chintalapudi, N., & Battineni, G. (2023). Multi-classification of lung infections using improved stacking convolution neural network. *Technologies*, *11*(5), 128.